JoVE: Science Education

MO Theory of Transition Metal Complexes

--Manuscript Draft--

Manuscript Number:	10447
Full Title:	MO Theory of Transition Metal Complexes
Article Type:	Manuscript
Section/Category:	Manuscript Submission
Corresponding Author:	Tamara Powers UNITED STATES
Corresponding Author Secondary Information:	
Corresponding Author's Institution:	
Corresponding Author's Secondary Institution:	
First Author:	Tamara Powers
First Author Secondary Information:	
Order of Authors:	Tamara Powers
Order of Authors Secondary Information:	

PI Name: Tamara M. Powers, Texas A&M University

Science Education Title: MO Theory of Transition Metal Complexes: Synthesis of $M(dppf)Cl_2$ (M = Ni, Pd).

Overview:

In this video, we will synthesize two metal complexes featuring the ligand 1,1'-bis(diphenylphosphino)ferrocene (dppf): $M(dppf)Cl_2$, where M = Ni or Pd. While both of these transition metal complexes are 4-coordinate, they exhibit different geometries at the metal center. Using MO theory in conjunction with ^1H NMR and Evan's method, we will determine the geometry of these two compounds.

Principles:

There are a variety of models that chemists use to describe bonding in molecules. It's important to remember that models are *representations* of systems and therefore have strengths but also important limitations. For example, Lewis dot structures, the simplest method for describing how atoms share electrons, do not take into account the geometry of the atoms in the molecule. Valence Shell Electron Pair Repulsion (VSEPR) theory does describe the geometry at atoms, but it does not provide an explanation for the observation that isoelectronic species that have the same number of valence electrons can exhibit different geometries. Especially for transition metal complexes, both of these models fall short in describing the bonding at metals. Crystal field theory is a bonding model that is specific to transition metal complexes. This model looks at the effect of a ligand's electric field on the *d* or *f* atomic orbitals of a metal center. The interaction results in a break in degeneracy of those atomic orbitals.

In this video, we will focus on molecular orbital (MO) theory, which is a powerful model that can be used to describe bonding in not only main group molecules, but is also suitable for modeling the bonding in transition metal complexes. Here, we will demonstrate how to generate an MO diagram of metal-containing compounds.

Molecular Orbital Theory

MO theory describes chemical bonding as the linear combination of the atomic orbitals (LCAO) of each atom in a given compound. The molecular orbitals (MOs) that results from LCAOs describe both the geometry and energy of the electrons shared by a number of atoms in the molecule (i.e. the directionality and strength of the bonds formed by given atoms).

To review basic MO theory that is covered in many general chemistry textbooks, let's first consider the diatomic molecule F_2 (full MO diagram in **Figure 1**). A fluorine atom has 4 valence atomic orbitals: 2*s*, $2p_x$, $2p_y$, and $2p_z$. The 2*s* orbital is lower in energy than the 2*p* atomic orbitals, which are all of the same energy. A linear combination of atomic orbitals will occur between atomic orbitals of similar energy and of matching symmetry. In this case, the 2*s* orbital on one F atom will interact with the 2*s* orbital on the other F atom.

Addition of these two orbitals results in the formation of a σ bonding MO (**Figure 1**). Bonding is a stabilizing interaction and therefore the resulting σ MO is lower in energy relative to the energy of the 2*s* atomic orbitals. Subtracting the 2*s* orbitals results in an anti-bonding interaction (destabilizing), designated as σ*, which is higher in energy relative to the 2*s* atomic orbitals (**Figure 1**).

Likewise, the 2*p* atomic orbitals will combine to form bonding and anti-bonding interactions. Like the 2*s* atomic orbitals, the $2p_z$ atomic orbitals (which lay along the F–F bond) form σ and σ* interactions. If we consider the $2p_x$ and $2p_y$ atomic orbitals, we see that they form different types of bonding and anti-bonding interactions called π and π* respectively (**Figure 1**). It is easy to differentiate between σ and π bonds because σ bonding orbitals are cylindrically symmetrical about the internuclear axis while π orbitals have a nodal plane along the internuclear axis. The spatial overlap between atomic orbitals that form σ bonds is greater than the spatial overlap between atomic orbitals that form π bonds. Therefore, the resulting π and π* MOs are less stabilized and destabilized, respectively, compared to the σ and σ* MOs formed by the $2p_z$ atomic orbitals. We can then fill the MOs with the valence electrons for the two F atoms.

Let's now consider a more complex molecule such as $[Co(NH_3)_6]Cl_3$ (**Figure 2**). If we used the same process as above (considering the atomic orbital overlap between 2 atoms at a time), generating an MO diagram of this molecule would be extremely challenging. Instead, we can use *group theory* to first generate a *symmetry adapted* linear combination (SALC) of the ligands. We can then use symmetry to determine the bonding/anti-bonding interactions that form between the atomic orbitals on the metal and the resulting SALCs.

To generate the SALCs for $[Co(NH_3)_6]^{3+}$, we follow a similar procedure outlined in the "Group Theory" video in the *Inorganic Chemistry* series:

1. Determine the point group of the molecule.
2. Generate a reducible representation of the ligand atomic orbitals.
3. Reduce the reducible representation to irreducible representations.

$[Co(NH_3)_6]^{3+}$ is in the point group O_h. Since we are only concerned about the bonding at the metal center, we can simply consider the 2*s* atomic orbitals on each NH_3 ligand. If we follow steps 1 – 3 for the N 2*s* orbitals we find that the reducible representation is $\Gamma_{red} = A_{1g} + E_g + T_{1u}$ (**Figure 2**). While the A_{1g} set represents 1 SALC, the E_g and T_{1u} sets actually represent 2 and 3 SALC s, respectively, giving a total of 6 SALCs (the same number of ligands in the cation $[Co(NH_3)_6]^{3+}$!). The 2 SALCs in the E_g set have the same symmetry and will result in degenerate MOs when they interact with the atomic orbitals of the Co (the same can be said about the 3 SALCs in the T_{1u} set). Using the character table in **Figure 2**, we can determine how the atomic orbitals of Co transform in the O_h point group. For example, the d_{z^2} and $d_{x^2-y^2}$ orbitals form an E_g set. Since we have 2 ligand SALCs with E_g symmetry, those SALCs will form bonding/anti-bonding interactions with the d_{z^2} and $d_{x^2-y^2}$ Co atomic orbitals. Continuing in the same fashion for all of the valence atomic orbitals of Co, we generate an MO diagram for the transition metal complex, shown in **Figure 3**. Notice that the remaining *d*-orbitals (d_{xz}, d_{yz}, and d_{xy}) transform as a set (T_{2g}) but do not have an appropriate symmetry matched SALC. These atomic orbitals therefore become "non-bonding"

molecular orbitals. In other words, they do not participate in bonding with the ligands in this transition metal complex.

Highlighted in **Figure 3** are the non-bonding *d*-orbitals and the σ* orbitals with *d*-orbital character. When this group of MOs is considered separately from the entire MO diagram it is referred to as the *d*-orbital splitting diagram of a transition metal complex. Since the *d*-orbital splitting diagram contains the HOMO and the LUMO, which are typically the most important orbitals to understand the chemistry and spectroscopy of coordination complexes, chemists will often refer to the *d*-orbital splitting diagram instead of the entire MO diagram. Conveniently, the *d*-orbital splitting diagram can be filled with the number of de^- on the metal center, since the ligand-based electrons always fill the σ-based MOs in the MO diagram.

Considering the d-orbital splitting diagrams for dppfMCl$_2$

Let's consider a simple 4-coordinate metal complex MX_4. MX_4 can exist in two geometries: tetrahedral or square planar. The *d*-orbital splitting diagrams for the point groups T_d (tetrahedral) and D_{4h} (square planar) is shown in **Figure 4**. While the general metal complexes M(dppf)Cl_2 do not have 4 equivalent ligands, and therefore are not in the point groups T_d or D_{4h}, we can still use these *d*-orbital splitting diagrams as a *model* to describe the *d*-orbital MOs for the two possible geometries.

Now, let's consider the *d*-electron count for M(dppf)Cl_2. Both Ni and Pd are in Group 10 of the periodic table. They both will therefore have the same oxidation state (2+) and *d*-electron count (d^8). If we fill the two *d*-orbital splitting diagrams above with 8 electrons, we see that the square planar geometry results in a diamagnetic complex while the tetrahedral MO diagram is consistent with a paramagnetic species. There are several factors that go into determining which geometry is energetically favored. In the square planar geometry, there are fewer electrons in anti-bonding orbitals, which would indicate that the square planar geometry is more *electronically* favored. However, we also need to consider the energy required to pair electrons. The electron pairing energy in square planar molecules is higher than that in tetrahedral molecules, which have fewer completely filled orbitals. Finally, we need to consider the amount the σ* *d*-orbitals are destabilized. Larger metal atoms have greater spacial overlap with ligands, resulting in higher energy σ* *d*-orbitals.

Finally, we also need to consider the energy contribution from steric repulsions. Tetrahedral geometry is more *sterically* favored (with angles of 109.5°) compared to square planar geometry (90°). Therefore, there are several opposing factors that affect which geometry is more favored given the identity of M in M(dppf)Cl_2.

We will be able to distinguish between these two geometries using NMR. If the molecule is square planar, we will observe a diagnostic ^{1}H NMR of a diamagnetic species. If the molecule is tetrahedral, we will observe paramagnetic signals in the ^{1}H NMR. Finally, we will use Evan's method (see the "*Evan's Method*" video for more details) to determine the solution magnetic moment of the paramagnetic species.

Procedure:

1. For safety precautions the Schlenk line safety should be reviewed prior to conducting the experiments. Glassware should be inspected for star cracks before using. Care should be taken to ensure that O_2 is not condensed in the Schlenk line trap if using liquid N_2. At liquid N_2 temperature, O_2 condenses and is explosive in the presence of organic solvents. If it is suspected that O_2 has been condensed or a blue liquid is observed in the cold trap, *leave the trap cold under dynamic vacuum. Do* ***NOT*** *remove the liquid N_2 trap or turn off the vacuum pump.* Over time the liquid O_2 will evaporate into the pump—it is only safe to remove the liquid N_2 trap once all of the O_2 has evaporated. See "Synthesis of a Ti(III) Metallocene Using Schlenk line Technique" video.[1]

   Setup of the Schlenk Line for the synthesis of Ni(dppf)Cl_2 and Pd(dppf)$_2Cl_2$ (for a more detailed procedure, please review the "Schlenk Lines Transfer of Solvent" video in the *Essentials of Organic Chemistry* series).

   1.1. Close the pressure release valve.

   1.2. Turn on the N_2 gas and the vacuum pump.

   1.3. As the Schlenk line vacuum reaches its minimum pressure, prepare the cold trap with either liquid N_2 or dry ice/acetone.

   1.4. Assemble the cold trap.

2. Synthesis of Ni(dppf)Cl_2 (**Figure 5**) under anaerobic/inert conditions. ~~"Synthesis of a Ti(III) Metallocene Using Schlenk line Technique" video.[2]~~ *NOTE:* While the synthesis of Ni(dppf)Cl_2 can be conducted in aerobic conditions, higher yields are obtained when conducted in anaerobic conditions.

   ~~1.1.~~2.1. Add 550 mg dppf (1 mmol) and 40 mL of isopropanol to a three-neck flask. *NOTE:* dppf can be purchased from Sigma Aldrich or synthesized using literature methods.[3]

   ~~1.2.~~2.2. Fit the center neck of the three-neck flask with a condenser and a vacuum adapter. Fit the two remaining necks with 1 glass stopper and 1 rubber septum.

   ~~1.3.~~2.3. Degas the solution by bubbling N_2 gas through the solvent for 15 minutes. Use the vacuum adapter at the top of the condenser as the "vent."

   ~~1.4.~~2.4. Connect the vacuum adapter at the top of the condenser to N_2 using the Schlenk line.

   ~~1.5.~~2.5. Begin heating the three-neck flask in a water bath set to 90 °C.

   ~~1.6.~~2.6. In a single neck round bottom flask, add 237 mg $NiCl_2$▪$6H_2O$ (1 mmol) to 4 mL of a 2:1 mixture of isopropanol (reagent grade) and methanol (reagent grade). Sonicate the resulting mixture until all of the Ni salt has dissolved (about 1 minute). NOTE: If a Sonicator is not available, gently heat the mixture in a water bath.

Commented [HK1]: I am just wondering, heating a water bath to 90 deg. Celsius for over two hours, doesn't it evaporate rather quickly? Why don't you use an oil bath? Is it something safety related?

~~1.7.~~2.7. Degas the Ni solution by bubbling N_2 gas through the mixture for 5 minutes.

~~1.8.~~2.8. Add the $NiCl_2$▪$6H_2O$ solution to the three-neck round bottom flask *via* cannula transfer.

~~1.9.~~2.9. Allow the reaction to reflux for 2 hours at 90 °C.

~~1.10.~~2.10. Allow the reaction to cool in an ice bath. Isolate the resulting green precipitate by vacuum filtration through a fritted funnel.

~~1.11.~~2.11. Wash the product with 10 mL of cold isopropanol, followed by 10 mL of hexanes.

~~1.12.~~2.12. Allow the product to air dry before preparing the NMR sample.

~~1.13.~~2.13. Take a ^1H NMR of the product in chloroform-*d*.

~~1.14.~~2.14. If the ^1H NMR is indicative of a paramagnetic species, prepare an NMR for Evan's method following the instructions in step 4.

~~2.~~3. Synthesis of $Pd(dppf)Cl_2$ (**Figure 6**).[1] Use standard Schlenk line techniques for the synthesis of $Pd(dppf)Cl_2$ (see the "Synthesis of a Ti(III) Metallocene Using Schlenk line Technique" video). *NOTE:* While the synthesis of $Pd(dppf)Cl_2$ can be conducted in aerobic conditions, higher yields are obtained when conducted in anaerobic conditions.

~~2.1.~~3.1. Add 550 mg (1 mmol) dppf and 383 mg (1 mmol) bis(benzonitrile)palladium(II) chloride to a Schlenk flask and prepare the Schlenk flask for the cannula transfer of solvent.

~~2.2.~~3.2. Add 20 mL of degassed toluene to the Schlenk flask *via* cannula transfer.

~~2.3.~~3.3. Allow the reaction to stir for at least 12 hours at room temperature.

~~2.4.~~3.4. Isolate the resulting orange precipitate by vacuum filtration through a fritted funnel.

~~2.5.~~3.5. Wash the product with toluene (10 mL), followed by hexanes (10 mL).

~~2.6.~~3.6. Allow the product to air dry before preparing the NMR sample.

~~2.7.~~3.7. Take a ^1H NMR of the product in chloroform-*d*.

~~2.8.~~3.8. If the ^1H NMR is indicative of a paramagnetic species, prepare an NMR for Evan's method following the instructions outlined in step 4.

~~3.~~4. Prepare the Evan's method sample. For a more detailed procedure, please refer to the "Evan's method" video.

~~3.1.~~4.1. In a scintillation vial, prepare a 50:1 (volume:volume) solution of chloroform-*d*:trifluorotoluene. Pipette 2 mL of deuterated solvent, and to this add 40 μL of trifluorotoluene. Cap the vial. *NOTE:* In this example, we will be using ^{19}F NMR to observe the shift of the F signal in trifluorotoluene in the presence of the paramagnetic species.

~~3.2.~~4.2. With this solution, prepare the capillary insert.

~~3.3.~~4.3. Weigh 10–15 mg of the paramagnetic sample into a new scintillation vial and note the mass.

~~3.4.~~4.4. Pipette ~600 μL of the prepared solvent mixture into the vial containing the paramagnetic species. Note the mass. Make sure that the solid completely dissolves.

~~3.5.~~4.5. In a standard NMR tube, carefully drop the capillary insert at an angle, as to not break it.

~~3.6.~~4.6. Pipette the solution containing the paramagnetic species into the NMR tube.

~~3.7.~~4.7. Acquire and save a standard ^{19}F NMR spectrum.

~~3.8.~~4.8. Note the temperature of the probe.

~~3.9.~~4.9. Note the radiofrequency.

Representative Results:

Commented [PTM2]: Spectra will be provided on day of filming

Pd(dppf)Cl$_2$:

^{1}H NMR (chloroform-*d*, 400 MHz, δ, ppm): 4.22 (alpha-H), 4.42 (beta-H), 7.89, 7.44, 7.54 (aromatic).[4]

Ni(dppf)Cl$_2$:

^{1}H NMR (chloroform-*d*, 300 MHz, δ, ppm): 20.85, 10.04, 4.23, 3.98, 1.52, –3.31, –7.10.

Evan's Method, looking at the ^{19}F shift of trifluorotoluene:

Commented [PTM3]: These values may change depending on what we do the day of filming.

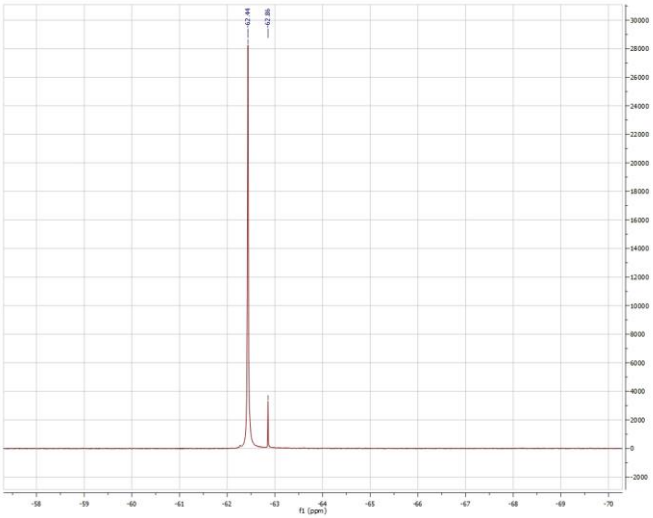

Observed μ_{eff} = 3.31 μ_b

Mass of the sample: 9.9 mg

Mass of solution (chloroform-*d* + trifluorotoluene): 0.9019 g

Temperature of probe: 295.1 K

NMR Field (MHz): 470.06

Reported μ_{eff} = 3.39 μ_b.[5]

For S = 1 (predicted based on tetrahedral geometry, **Figure 4**), theoretical μ_{eff} = 2.83 μ_b.

For S = 3/2, theoretical μ_{eff} = 3.46 μ_b.

Discussion of Results

Based on the ^{1}H NMR data, we see that Pd(dppf)Cl_2 is diamagnetic and therefore exhibits square planar geometry. The ^{1}H NMR of Ni(dppf)Cl_2 is paramagnetic and therefore is tetrahedral at the Ni center. Evan's method confirms that Ni(dppf)Cl_2 is paramagnetic, exhibiting a solution magnetic moment of 3.31 μ_b, which is close to the literature reported value for this compound. Since Ni is small, the sterics outweighs any electronic stabilization associated with square planar geometry, making Ni(dppf)Cl_2 tetrahedral. On the other hand, Pd is large and, therefore, has higher energy σ* *d*-orbitals. In this case, the electronic stabilization greatly outweighs the steric repulsions, resulting in a square planar geometry at Pd in Pd(dppf)Cl_2.

Summary:

In this video we learned how MO theory can be used as a model of the bonding in transition metal complexes. We synthesized two complexes with the general formula M(dppf)Cl_2. When M = Ni, the 4-coordinate complex exhibits a tetrahedral geometry. Replacing the Ni atom with a larger transition metal (Pd), the molecule takes on square planar geometry.

Applications:

Previously, we learned about the important role ferrocene plays in the field of organometallic chemistry. Substituted ferrocenes, including dppf, are used as chelating ligands for 1st, 2nd, and 3rd row transition metals. The resulting complexes are used in homogeneous catalysis (*i.e.*, [1,1'-bis(diphenylphosphino)ferrocene]palladium(II) dichloride, Pd(dppf)Cl_2, is a catalyst for C–C and C–heteroatom bond-forming reactions).

Understanding the bonding in transition metal complexes is important for explaining their structure and reactivity. One of the strengths of MO theory is that it provides a good model that can be used to explain the reactivity of transition metal complexes. In many cases, the metal center is the location of any reactivity exhibited by the molecule. Therefore, it is valuable to have a picture of the electron density at the metal center, which is summarized in the *d*-orbital splitting diagram derived from MO theory (**Figure 3**). Notice that not only do the MOs in the *d*-orbital splitting diagram exhibit mostly *d*-orbital character (the σ* orbitals are closest in energy to the atomic *d*-orbitals of the metal and therefore most of the electron density in those MOs is centered on the metal atom) but that the splitting diagram also contains the HOMO and LUMO of the molecule. Therefore, any chemistry that occurs will directly affect the *d*-orbital splitting diagram of the molecule.

Legend:

Figure 1. MO diagram of F_2.

Figure 2. Linear combination of ligand atomic orbitals of $[Co(NH_3)_6]Cl_3$.

Figure 3. MO diagram for $[Co(NH_3)_6]Cl_3$.

Figure 4. The *d*-orbital splitting diagrams for the point groups T_d (tetrahedral) and D_{4h} (square planar).

Figure 5. Synthesis of Ni(dppf)Cl_2.

Figure 6. Synthesis of Pd(dppf)Cl_2.

References

[1] Corain, B.; Longato, B.; Favero, G. Heteropolymetallic Complexes of 1,1'-Bis(diphenylphosphino)ferrocene (dppf). III*. Comparative Physicochemical Properties of (dppf)MCl_2 (M = Co, Ni, Pd, Pt, Zn, Cd, Hg). *Inorg. Chim. Acta*. **1989**, *157*, 259-266.

[3] Cullen, W. R.; Einstein, F. W. B.; Jones, T.; Kim, T.-J. Structures of three hydrogenation catalysts [(P-P)Rh(NBD)]ClO_4 and some comparative rate studies where (P-P) = (η^5-

$R_1R_2PC_5H_4)(\eta^5\text{-}R_3R_4PC_5H_4)Fe$ ($R_1 = R_2 = R_3 = R_4 = Ph$; $R_1 = R_2 = Ph$, $R_3 = R_4 = CMe_3$; $R_1 = R_3 = Ph$, $R_2 = R_4 = CMe_3$) *Organometallics* **1983**, *4*, 346-351.

[4] Colacot, T. J.; C.-Olivares, R.; H.-Ortega, S. Synthesis, X-ray, spectroscopic and a preliminary Suzuki coupling screening studies of a complete series of $dppfMX_2$ (M = Pt, Pd; X = Cl, Br, I) *J. Organomet. Chem.* **2001**, *637-639*, 691-697.

[5] Rudie, A. W.; Lichtenberg, D. W.; Katcher, M. L.; Davison, A. Comparative Study of 1,1'-bis(diphenylphosphino)cobaltocinium hexafluorophosphate and 1,1'-bis(dipenylphosphino)ferrocene as Bidentate Ligands. *Inorg. Chem*. **1978**, 17, 2859-2863.

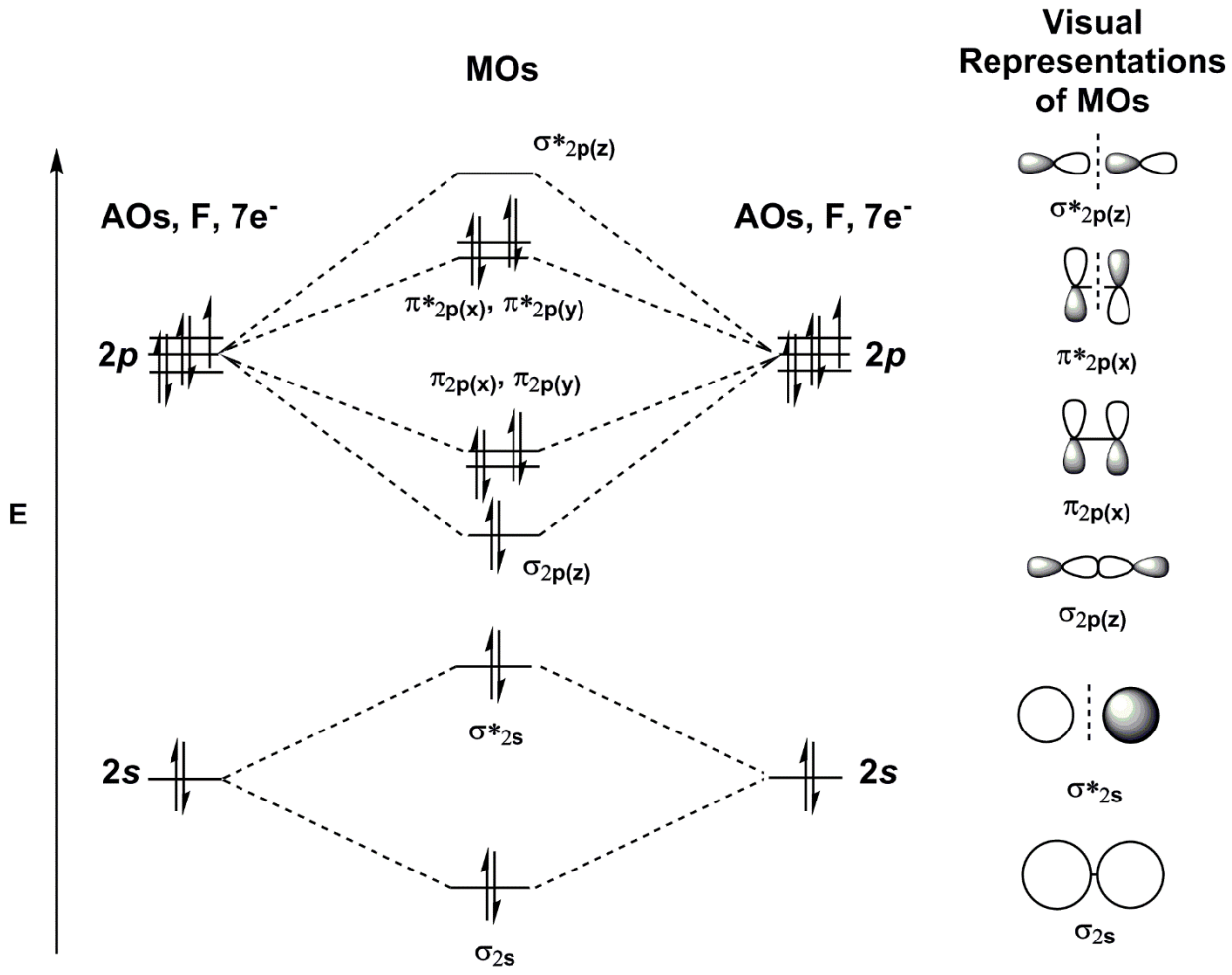

Figure 1.

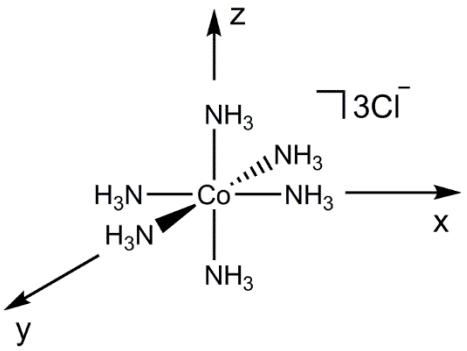

O_h	E	$8C_3$	$6C_2$	$6C_4$	$3C_2'$	i	$6S_4$	$8S_6$	$3\sigma_h$	$3\sigma_d$		
A_{1g}	1	1	1	1	1	1	1	1	1	1		$x^2+y^2+z^2$
A_{2g}	1	1	-1	-1	1	1	-1	1	1	-1		
E_g	2	-1	0	0	2	2	0	-1	2	0		$(2z^2-x^2-y^2, x^2-y^2)$
T_{1g}	3	0	-1	1	-1	3	1	0	-1	-1	(R_x, R_y, R_z)	
T_{2g}	3	0	1	-1	-1	3	-1	0	-1	1		(xz, yz, xy)
A_{1u}	1	1	1	1	1	-1	-1	-1	-1	-1		
A_{2u}	1	1	-1	-1	1	-1	1	-1	-1	1		
E_u	2	-1	0	0	2	-2	0	1	-2	0		
T_{1u}	3	0	-1	1	-1	-3	-1	0	1	1	(x, y, z)	
T_{2u}	3	0	1	-1	-1	-3	1	0	1	-1		
Γ_{red}	6	0	0	2	2	0	0	0	4	4		

$\Gamma_{red} = A_{1g} + E_g + T_{1u}$

Figure 2.

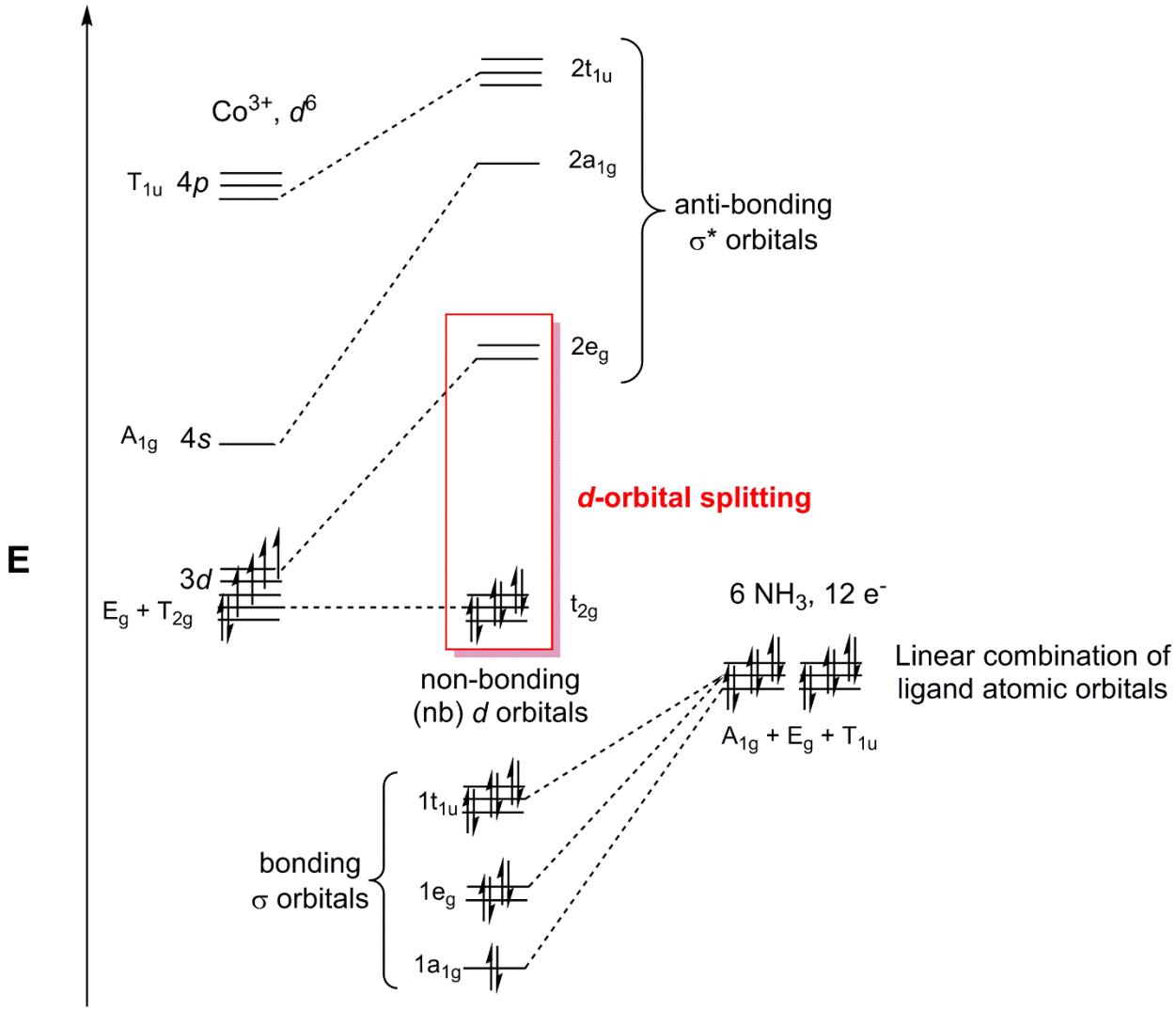

Figure 3.

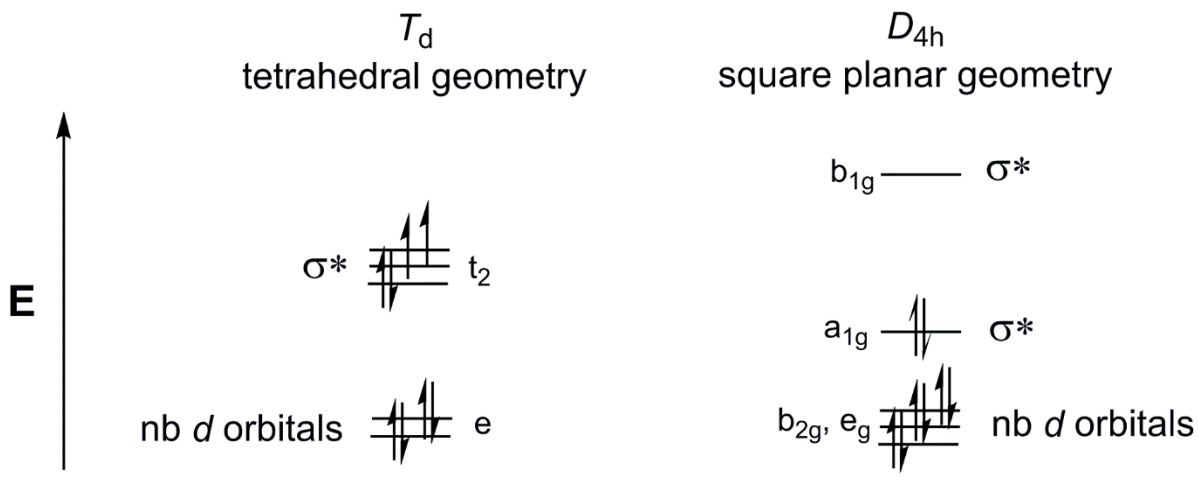

Figure 4.

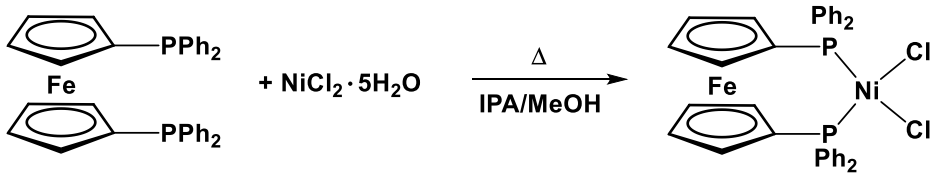

Figure 5.

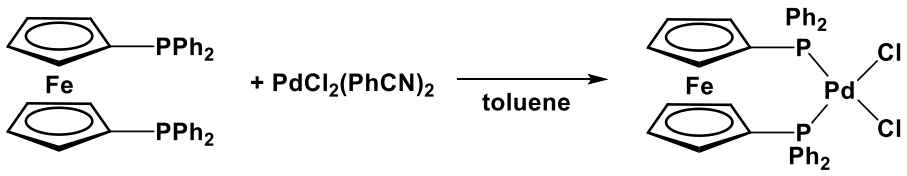

Figure 6.